

ARTHRITIS & RHEUMATOLOGY

Full Length

NF- κ B2 Controls Migratory Activity of Memory T Cells by Regulating Expression of CXCR4 in A Mouse Model of Sjögren's Syndrome

Mie Kurosawa,¹ Rieko Arakaki,¹ Akiko Yamada,¹ Takaaki Tsunematsu,² Yasusei Kudo,¹ Jonathan Sprent,³ and Naozumi Ishimaru¹

Supported by JSPS KAKENHI (grants 16H02690 to Dr. Ishimaru).

¹Mie Kurosawa, BS, Rieko Arakaki, PhD, Akiko Yamada, DDS, PhD, Yasusei Kudo, DDS, PhD, Naozumi Ishimaru, DDS, PhD: Department of Oral Molecular Pathology, Tokushima University Graduate School of Biomedical Sciences, Tokushima, Japan; ²Takaaki Tsunematsu, DDS, PhD: Department of Pathology and Laboratory Medicine, Tokushima University Graduate School of Biomedical Sciences, Tokushima, Japan; ³Jonathan Sprent, MD, PhD: Immunology Research Program, Garvan Institute of Medical Research, New South Wales, Australia

Address corresponded to Naozumi Ishimaru, DDS, PhD, Department of Oral Molecular Pathology, Tokushima University Graduate School of Biomedical Sciences, 3-18-15 Kuramoto, Tokushima, 770-8504, Japan. E-mail: ishimaru.n@tokushima-u.ac.jp

Keywords: Autoimmunity, TEM cell, Migration, CXCL12, CXCR4, CXCR7, TGF β , TGF β R, Sjögren's syndrome

Abbreviations: TEM cell, effector memory T cell; CXCL, C-X-C motif chemokine ligand; CXCR, C-X-C chemokine receptor; NF- κ B, nuclear factor- κ B; TGF β , transforming growth factor β ; TGF β R, TGF β receptor; aly, alymphoplasia; SS, Sjögren's syndrome.

Objective. Dysregulated chemokine signaling contributes to autoimmune diseases by facilitating aberrant T-cell infiltration into target tissues, but the specific cytokines, receptors, and T-cell populations remain largely unidentified. Role of the potent chemokine CXCL12 and its receptor CXCR4 in T-cell autoimmune response was examined using alymphoplasia (*aly*)/*aly* mice, a Sjögren's syndrome (SS) model.

Methods. T-cell phenotypes in the salivary gland of *aly/aly* mice were evaluated using immunological analysis. *In vitro* migration assay was used to assess T-cell migratory activity toward several chemokines. Gene expression of chemokine receptors, and transforming growth factor (TGF) β receptors was measured with quantitative reverse transcription-polymerase chain reaction. The CXCR4 antagonist AMD3100 was administered to the *aly/aly* mice to evaluate its suppressive effect on autoimmune lesions.

Results. Effector memory T (TEM) cells derived from *aly/aly* mice demonstrated higher *in vitro* migratory activity toward CXCL12 than *aly/+* TEM cells. CXCL12 expression was specifically upregulated in the SS target cells of *aly/aly* mice. TEM cells from *RelB*^{-/-} mice, but not nuclear factor (*NF*)- κ *B1*^{-/-} mice, also showed high migratory activity toward CXCL12, implicating a nonclassical NF- κ B2/RelB pathway in the regulation of TEM cell migration. TEM cells from *aly/aly* mice also overexpressed TGF β receptors I and II. The CXCR4 antagonist AMD3100 suppressed autoimmune lesions in *aly/aly* mice by reducing TEM cell infiltration.

Conclusion. Our results suggest that the NF-κB2/RelB pathway regulates T-cell migration to autoimmune targets through TGF β /TGF β R-dependent regulation of CXCL12–CXCR4 signaling. This suggests that these signaling pathways are potential therapeutic targets for treating autoimmune diseases.

INTRODUCTION

Chemokines are important activators of adhesion molecules and drivers of lymphocyte migration to inflammatory sites, including autoimmune lesions. Activated or autoreactive T cells derived from naïve T cells migrate to and attack self-tissue or cells in the initiation of autoimmunity (1,2). T-cell migration, differentiation, and effector activity are controlled by several chemokines, including CXCL9, CXCL10, CXCL11, and CXCL12 (2-6). However, as T cells dynamically express multiple chemokine receptors and chemokine binding overlaps among these receptors, the precise mechanisms of T-cell regulation by chemokine/receptor signaling remain unclear.

Among these chemokines, CXCL12 is a critical regulator of tissue homeostasis, immune surveillance, and inflammatory responses (7). CXCL12 can bind to two receptors on T cells, CXCR4 and CXCR7. Moreover, CXCR7 directly modulates CXCR4 signaling via CXCR7–CXCR4 heterodimerization (7). When CXCL12 binds to CXCR4 on T cells, CXCR4 heterodimerizes with the T-cell receptor to stimulate multiple phospholipase C isoforms, increasing intracellular calcium concentration and activating the extracellular signal-regulated kinase pathway, thereby initiating the transcription of genes associated with specific T-cell functions (8). In cancer cells, expression of CXCR4 and CXCR7 is regulated by nuclear factor (NF)-κB (9), but it is unclear how cytokine receptor expression in peripheral T cells is controlled.

NF-κB plays a key role in the regulation of many inflammatory processes of immune cells (10). The NF-κB family consists of five subunits: NF-κB1 (p105–p50),

NF-κB2 (p100–p52), RelA (p65), RelB, and c-Rel. Hetero- or homo-dimers of these subunits can be translocated into the nucleus to bind κB sequences neighboring target genes (11). Two NF-κB signaling pathways exist in the immune cells, a “classical” pathway initiated by the NF-κB1–RelA complex, and an alternative “nonclassical” pathway initiated by the NF-κB2–RelB complex (11). The importance of NF-κB-inducing kinase (NIK) in NF-κB activation has been demonstrated in studies using NIK-deficient and alymphoplasia (*aly*)/*aly* mice (12-15).

The *aly/aly* mice carry a mutation in the NIK/mitogen-activated protein kinase kinase kinase 14 (MAP3K14) gene. NIK/MAP3K14 is key in regulating the processing of p100 to p52 through IKK α in hematopoietic cells (12-15). In addition, the *aly/aly* mouse exhibits autoimmune lesions in the lacrimal and salivary glands, resembling those observed in patients with Sjögren’s syndrome (SS) (16). We previously reported that the abnormal activation of naïve T cells, but not effector memory T (TEM) cells, in *aly/aly* mice contributes to the onset of autoimmunity due to impaired crosstalk between the NF-κB subunits (17). However, the precise role of NIK in TEM cell function still remains unclear. In particular, although the chemokine-dependent migration of TEM cells to the target organs of autoimmunity via the NF-κB2 signaling pathways, including NIK, is a key mechanism in the development of autoimmunity, but the precise contribution of NIK remains to be explored.

The heterogeneity of memory T cells depends on surface molecule expression profile, effector function, signal transduction, and location (18,19). Three distinct subsets of memory T cells have been identified: central memory T cells, TEM cells, and

memory stem T cells (20). Central memory T cells express CD62L (L-selectin) and CCR7 (20), whereas TEM cells do not (20,21). The precise migratory function of TEM cells to the target organ in autoimmunity needs to be explored.

In the present study, we focused on the migratory response of T cells to chemokines in *aly/aly* mice and the molecular mechanism underlying the expression of chemokine receptors. Our results indicate a yet unreported role of NF- κ B2 signaling in TEM cell function, to our knowledge, and in the pathogenesis of autoimmune diseases.

MATERIALS AND METHODS

Mice. The *aly/aly* and *aly/+* mice were obtained from CLEA Japan. *NF-κB1*^{-/-} and *RelB*^{-/-} mice were obtained from the Jackson Laboratory. The genetic background of their mice is C57BL/6J. The mice were housed in a pathogen-free environment within the animal facility in Tokushima University. Mice that were 6–16 weeks of age were used in the study, and all animal experiments were conducted according to the Fundamental Guidelines for Proper Conduct of Animal Experiment and Related Activities in Academic Research Institutions under the jurisdiction of the Ministry of Education, Culture, Sports, Science and Technology of Japan. The protocol was approved by the Committee on Animal Experiments of the University of Tokushima and Biological Safety Research Center (Permit Number: T27-7). All experiments were performed after administering anesthesia, and all efforts were made to minimize suffering.

Histological analysis. Salivary and lacrimal glands (SGs and LGs) were

harvested from the mice, were fixed in 10% phosphate-buffered formaldehyde (pH 7.2), and were prepared for histological examination by staining with hematoxylin and eosin (H&E).

Immunofluorescence staining and immunohistochemistry. Frozen sections of SG tissue were fixed with methanol/acetone (1:1), blocked using an avidin/biotin blocking kit (Vector Laboratories, Inc.) and 5% bovine serum albumin, and stained with biotinylated anti-mouse CD4 monoclonal antibody (mAb) (eBioscience, RM4.5), with Alexa fluoro-546 streptavidin (Invitrogen) as the second Ab. In addition, to detect CXCL12 expression in frozen LG tissues, anti-CXCL12 polyclonal Ab (anti-SDF1 α , Abcam), phycoerythrin (PE)-conjugated ant-mouse EpCAM (CD326) mAb (eBioscience, G8.8), PE-conjugated anti-CD45.2 mAb (BioLegend, 104), and biotin-conjugated anti-PE mAb (eBioscience, eBioPE-DLE) as the second Ab. After washing three times with PBS, nuclear DNA was stained with 4',6-diamidino-2-phenylindole dihydrochloride (DAPI) (Invitrogen). The sections were observed using a PASCAL confocal laser-scanning microscope (LSM: Carl Zeiss) at a magnification of 400 or 630 \times . LSM image browser version 3.5 (Carl Zeiss) was used for image acquisition. For immunohistochemical analysis, paraffin-embedded sections using the tissues fixed in 10% phosphate-buffered formaldehyde (pH 7.2) were stained with anti-CXCL12 polyclonal Ab (Abcam) using the biotin–avidin immunoperoxidase complex reagent (Dako) and 3,3'-diaminobenzidine (DAB) chromogen (Dako). The nuclei were counterstained with hematoxylin.

Enzyme-linked immunosorbent assay (ELISA). Serum concentration of

CXCL12 in B6, *aly*/+, and *aly*/*aly* mice was measured using mouse CXCL12/stromal cell-derived factor-1 (SDF-1) α Quantikine ELISA kit (R&D Systems Inc.).

Cell isolation. Spleen cells were suspended by homogenization and red blood cells were removed with 0.83% ammonium chloride. The remaining cells were washed twice with 2% fetal bovine serum/Dulbecco's modified Eagle's medium. CD44^{high} CD62L⁻ TEM and CD44^{low}CD62L⁺ naïve CD4⁺ T cells were isolated using a cell sorter (JSAN Jr Swift, Bay Bioscience) as shown in Supplementary Figure 1. The isolated cells were confirmed by the C-C chemokine receptor (CCR)7 expression (CCR7⁻ for TEM cells, CCR7^{low} for naïve cells) (Supplementary Figure 1). Lymphocytes infiltrating into the target organs were isolated by dispersing LG and SG tissues with 1 mg/ml collagenase solution (Wako), followed by a density-gradient centrifugation using Histopaque-1083 (Sigma-Aldrich).

Flow cytometric analysis. Lymphocytes from spleen and target organs were stained using antibodies against PE-Cy7-conjugated anti-mouse CD4 mAb (TONBO Biosciences, GK1.5), FITC-conjugated anti-mouse CD8 mAb (eBioscience, 53-6.7), PE-Cy5.5-conjugated anti-mouse CD44 mAb (TONBO Biosciences, IM7), APC-Cy7-conjugated anti-mouse CD62L mAb (BioLegend, Mel-14), PE-conjugated anti-mouse/human CXCR7 mAb (BioLegend, 8F11-M16), biotinylated anti-mouse CXCR4 mAb (eBioscience, 2B11), biotinylated anti-mouse CCR7 mAb (eBioscience, 4B12), APC-conjugated anti-mouse transforming growth factor β receptor I (TGF β RI, R&D systems, 141231), APC-conjugated anti-mouse TGF β RII polyclonal Ab (R&D systems), and APC-conjugated streptavidin (eBioscience). A FACScan flow cytometer

(BD Biosciences) was used to identify the cell populations according to surface expression profile. Data were analyzed using FlowJo FACS Analysis software (Tree Star Inc.).

In vitro chemotactic migration assay. After serum starvation in RPMI 1640 medium for 24 h, CD4⁺ T cells were plated (5×10^5 cells in 350 µl) in the culture plates insert (3.0-µm pore size, Merck Millipore). An equal volume of medium containing CXCL9, 10, 11, and 12 (0–750 ng/ml; R&D Systems Inc.) was added to the lower chamber in 350 µl of RPMI 1640 containing 0.1% BSA, and then the cells were cultured for 4 h at 37°C. The number of migrated cells was analyzed by flow cytometry.

Quantitative reverse transcription-polymerase chain reaction (qRT-PCR).

Total RNA was extracted from lymphocytes using the RNeasy mini kit (QIAGEN) and subsequently reverse-transcribed into cDNA. Ct values of > 35 cycles were discarded. For standardization, the Ct cutoff of all analyses was set at the default setting (0.2). The expression of mRNAs encoding CXCR4, CXCR7, CXCL12, TGFβRI, -II, -III, β-actin, and glycerol-3-phosphate dehydrogenase (GAPDH) was determined using a PTC-200 DNA Engine Cycler (Bio-Rad Laboratories) with SYBR Premix Ex Taq reagent (Takara Bio Inc.). The primer sequences used were as follows: CXCR4, forward, 5'-TCAGTGGCTGACCTCCTCTT-3' and reverse, 5'-TTTCAGCCAGCAGTTCCCTT-3'; CXCR7, forward, 5'-GGTCAGTCTCGTGCAGCATA-3' and reverse, 5'-GTGCCGGTGAAGTAGGTGAT-3'; CXCL12: forward, 5'-CTTCATCCCCATTCTCCTCA-3' and reverse,

5'-GACTCTGCTCTGGTGGAAAGG-3', TGF β receptor I (TGF β RI): forward,
5'-AACTGAAACACCGTGGAAC-3' and reverse,
5'-TGGGAAGCTTCAGTTGACC-3'; TGF β RII: forward,
5'-CCCAGTCTGGAAATGAAAGC-3' and reverse,
5'-ACTTTGTCGTGGGTTCTGG-3'; TGF β RIII: forward,
5'-TCAGATTGTGCCTGTCTCG-3' and reverse,
5'-CTGGGTGTTCTGCATTGTG-3'; β -actin: forward,
5'-GTGGGCCGCTCTAGGCACCA-3' and reverse,
5'-CGGTTGGCCTTAGGGTTCAGGGGGG-3', GAPDH: forward,
5'-TGCACCACTGCTTAC-3' and reverse,
5'-GGATGCAGGGATGATGTT-3'. To confirm the specificity of the primers, each PCR product was electrophoresed on an agarose gel to determine the DNA size (bp), and a single band for each product was detected at the expected size. Relative mRNA expression of each transcript was normalized against β -actin mRNA. To confirm the normalization by β -actin, the mRNA expression of CXCL12 was quantified using GAPDH as another housekeeping gene (Supplementary Figure 2B). The triplicates per experiment were analyzed. The qRT-PCR experiments were repeated at least three times.

Administration of AMD3100. The CXCR4 inhibitor AMD3100 octahydrochloride (5 mg/kg; Sigma) was administered daily to female *aly/aly* mice from 8 to 16 weeks of age by intraperitoneal (ip) injection. As a control, PBS was administered to *aly/aly* mice following the same regimen.

Statistical analysis. Means of each group were compared using unpaired Student's *t*-test. A probability (*p*) value of < 0.05 was considered statistically significant.

RESULTS

TEM cells in autoimmune lesions of *aly/aly* mice. Inflammatory lesions in the SG of *aly/aly* mice were observed from approximately 10 weeks of age as previously described (16). Infiltration of mononuclear cells around dilated ducts and the destruction or atrophy of acinar cells was found in the SG tissues harvested from 3 months old *aly/aly* mice (Figure 1A). Moreover, to evaluate the dysfunction of target organs, the flow volume of tear and saliva was measured. The flow in *aly/aly* mice was significantly lower than that in *aly/+* mice with respect to the autoimmune lesions in target organs (Supplementary Figure 2A). Immunofluorescence analysis revealed that CD4⁺ T cells were the predominant infiltrating cell type (Figure 1B), and flow cytometric analysis of isolated SG lymphocytes confirmed that over 80% were CD4⁺ T cells (Figure 1C and D). The number of CD44^{high}CD62L⁻CD4⁺ TEM cells was higher in the spleen of *aly/aly* mice than that in the *aly/+* mice, while there was no difference in the total number of TEM cells (Figure 1E) and in the number and proportion of CD44^{low}CD62L⁺ naïve CD4⁺ T cells in the spleen between *aly/aly* and *aly/+* mice (Figure 1E and F). By contrast, the number of both TEM and naive T cells in the SG increased significantly compared with that in *aly/+* mice (Figure 1F).

Enhanced migratory response of *aly/aly* mouse CD4⁺ T cells to CXC

chemokines. To examine whether the facilitation of migratory activity contributes to TEM cell infiltration observed in *aly/aly* mice, the migratory response of CD4⁺ T cells isolated from *aly/aly* and *aly/+* mouse spleen toward CXCL9, 10, 11, and 12 was evaluated by *in vitro* transwell migration assay. The migratory rates of *aly/aly* CD4⁺ TEM cells toward CXCL12 were significantly higher than those of *aly/+* TEM cells, while there was no difference in the migratory response to CXCL9, 10, and 11 (Figure 2A). Furthermore, the response increased with CXCL12 concentration (Figure 2C). In contrast, no migratory response toward any of these cytokines was observed with respect to naïve CD4⁺ T cells isolated from *aly/aly* and *aly/+* mouse spleen (Figure 2B and D).

Elevated CXCL12 expression in target tissues of *aly/aly* mice. We measured serum CXCL12 concentration by ELISA to examine whether higher serum concentration contributes to greater TEM cell migration/infiltration in *aly/aly* mice, but found no difference in the B6, *aly/+*, and *aly/aly* mice (Figure 3A). We then examined whether local accumulation of CXCL12 in the spleen or target organs is responsible for this enhanced migratory capacity of *aly/aly* TEM cells by measuring CXCL12 mRNA expression with qRT-PCR. CXCL12 mRNA expression in SGs and LGs of *aly/aly* mice was significantly higher than in *aly/+* SGs and LGs (Figure 3B and Supplementary Figure 2B), but it was not different in the spleen and lung (Figure 3B). These findings suggest that increased CXCL12 expression in the target tissues (SG and LG) contributes to the higher TEM cell accumulation and the consequent autoimmune response. It is known that increased chemokine levels are detectable in the inflamed tissues of SS

patients (22,23), and CXCL12 is ubiquitously expressed in many tissues and cell types (7). To determine the cell type producing CXCL12 in the target organs, immunofluorescence analysis was performed. CXCL12-expressing cells in target tissue of *aly/aly* mice at 12 weeks of age. EpCAM⁺ epithelial cells in LGs expressed CXCL12 in *aly/aly*, but not *aly/+*, mice while Ly5.2⁺ lymphocytes infiltrated in LGs didn't express CXCL12 in *aly/aly* mice (Figure 3C and D). The CXCL12 expression was found in the epithelial cells neighboring the area of lymphocyte infiltration (Figure 3C, D). At 6 weeks of age, when inflammatory lesions were absent, there was no difference in the CXCL12 expression in the LGs of *aly/aly* and *aly/+* mice (Supplementary Figure 2C), suggesting that CXCL12 expression by target cells increases along with the migration of inflammatory cells including T cells, and that T-cell migration may further increase following the upregulation of CXCL12, leading to the development of severe autoimmune lesions. Although the precise mechanism underlying CXCL12 upregulation in the target organs in *aly/aly* mice remains unclear, the production might be enhanced in the inflammatory lesions of target organs in *aly/aly* mice.

Elevated CXCL12 receptor expression on the TEM cells of *aly/aly* mice.

While CXCR4 is the best described CXCL12 receptor, this cytokine also binds to CXCR7 (7,24). To examine whether the upregulation of these receptors also contributes to enhanced CXCL12-dependent tissue infiltration of TEM cells in *aly/aly* mice, CXCR4 and CXCR7 expression in TEM and naïve T cells isolated from the mouse spleen were measured by flow cytometry. Surface expression of CXCR4 on TEM cells belonging to the *aly/aly* mice was significantly higher than that on *aly/+* TEM cells,

whereas no difference in the expression of CXCR7 was seen (Figure 4A and Supplementary Figure 3). By contrast, there was no difference in CXCR7 or CXCR4 expression on naïve CD4⁺ T cells between *aly/aly* and *aly/+* mice (Figure 4B). Furthermore, mRNA expression of CXCR4 was significantly higher in TEM cells isolated from the spleen of *aly/aly* mice compared with the *aly/+* mice, while there was no difference in CXCR7 mRNA expression (Figure 4C). No difference in the CXCR7 and CXCR4 expression in naïve CD4⁺ T cells was observed between *aly/aly* and *aly/+* mice (Figure 4D). These findings suggest that the high migratory activity of TEM cells from *aly/aly* mice toward CXCL12 results from the increased expression of CXCR4.

To understand the role of both classical and nonclassical NF-κB pathways in the migratory response of TEM cells to CXCL12, the *in vitro* migratory assay in response to CXCL12 was performed using TEM and naïve CD4⁺ T cells isolated from wild-type (WT), *NF-κB1 (p50)*^{-/-}, *aly/aly*, and *RelB*^{-/-} mice. There was no difference in the migratory response of TEM cells in WT and *NF-κB1*^{-/-} mice (Figure 4E). In contrast, *RelB*^{-/-} mice demonstrated a significantly increased migratory response without CXCL12 compared with the WT mice (Figure 4E). In addition, the migratory response to CXCL12 in *RelB*^{-/-} mice was significantly higher than that in the WT mice (Figure 4E). Moreover, the migratory response to CXCL12 in *RelB*^{-/-} mice was significantly higher than that in the *aly/aly* mice (Figure 4E). Therefore, TEM cells in *RelB*^{-/-} mice are generally more mobile to chemokines. In accordance with these results, no substantial migratory response was observed with respect to the naïve T cells in *NF-κB1*^{-/-}, *aly/aly*, and *RelB*^{-/-} mice (Figure 4F). This suggests that the nonclassical

NF-κB2/RelB pathway regulates the migratory response to CXCL12 in TEM cells.

Role of TGFβ1 in CXCR4 expression by TEM cells. TGFβ is considered as the master regulator of T-cell activity, and CXCR4 expression in human T cells is controlled by TGFβ1 (25,26). Therefore, we examined whether TGFβ1 signaling is involved in CXCR4 overexpression by *aly/aly* TEM cells. TGFβ1 upregulated the expression of CXCR4 mRNA in both *aly/aly* and *aly/+* TEM cells, but the increase was greater only in *aly/aly* TEM cells (Figure 5A). By contrast, no enhancement of CXCR4 mRNA expression by TGFβ1 was observed in naïve CD4⁺ T cells of either genotype (Figure 5A). Moreover, the protein levels of CXCR4 expression in TEM cells of *aly/aly* mice increased significantly because of TGFβ1, whereas an increase in CXCR4 expression on TEM cells of *aly/+* mice was not observed (Figure 5B). There was no change in CXCR4 expression in naïve T cells by TGFβ1 in both *aly/aly* and *aly/+* mice (Figure 5B). Consistent with a critical role of CXCL12–CXCR4 signaling during increased *aly/aly* TEM cell migration, the migratory response of *aly/aly* TEM cells to CXCL12 was further upregulated by TGFβ1, compared with *aly/+* TEM cells (Figure 5C). Collectively, these results suggest that NF-κB2 negatively controls CXCR4 expression through TGFβ signaling.

We also investigated whether TGFβ receptor signaling is upregulated in *aly/aly* TEM cells, thereby accounting for the enhanced sensitivity to TGFβ. Indeed, qRT-PCR results showed that the expression of TGFβRI and II was significantly higher in *aly/aly* TEM cells than in *aly/+* TEM cells (Figure 5D). As expected, there was no difference in the expressions by naïve CD4⁺ T cells in *aly/+* and *aly/aly* mice, again consistent with

the lack of TGF β effects on migration (Figure 5D). There was also no difference in TGF β RIII expression in *aly/+* and *aly/aly* TEM cells (Figure 5D). Furthermore, flow cytometric analysis revealed that the number of TGF β RI $^+$ TEM cells in *aly/aly* mice was significantly higher than that in *aly/+* mice (Figure 5E). The proportion of TGF β RII $^+$ TEM cells in *aly/aly* mice also increased compared with that in *aly/+* mice (Figure 5F). These findings suggest that NF- κ B2 controls the migratory function of TEM cells by regulating the TGF β /TGF β R/CXCR4 signaling axis.

Therapeutic effect of CXCR4 inhibitor on autoimmune lesions in *aly/aly* mice. Finally, we examined whether the suppression of migration-promoting signaling pathways reduces the autoimmune response in *aly/aly* mice. Intraperitoneal injection of the specific CXCR4 antagonist AMD3100 from 8 to 16 weeks of age dramatically reduced autoimmune lesions in SG and LG of *aly/aly* mice and suppressed lymphocyte infiltration into these target organs (Figure 6A and B). Moreover, the proportion of TEM cells among all infiltrated lymphocytes in SG and LG was significantly reduced by AMD3100 compared with that in the vehicle-treated controls (Figure 6C and D). There were no differences in the number of CD3 $^+$ T cells, CD19 $^+$ B cells, CD4 $^+$ T cells, and CD8 $^+$ T cells in the spleen of mice administered with AMD3100 or vehicle (Supplementary Figure 4). This suggests that inhibition of CXCR4 prevents autoimmune lesions in *aly/aly* mice by suppressing CXCL12-induced TEM cell migration.

DISCUSSION

In this study, the phenotype of the CD4⁺ T cells infiltrating into the target tissues of *aly/aly* mice was similar to that of CD44^{high}CD62L⁻CCR7⁻ CD4⁺ TEM cells. These infiltrating cells are believed to involve autoreactive T cells. Our findings strongly suggest that CXCL12 is a critical factor promoting TEM cell infiltration into target organs. The migratory response of TEM cells, including autoreactive T cells, was markedly enhanced in *aly/aly* mice compared with *aly/+* mice. Several reports have demonstrated that chemokines are upregulated in the target organs in patients with SS (22,27), and indeed, CXCL12 expression increased in the inflammatory lesions of *aly/aly* mice. Moreover, CXCR4 was also upregulated in the TEM cells of the *aly/aly* mice, thus explaining the strong recruitment of these cells into the target tissues.

CXCR4 is one of several chemokine receptors exploited by the human immunodeficiency virus (HIV) to infect CD4⁺ T cells in addition to a major receptor of CXCL12, called SDF-1 (28). CXCR4 is widely expressed at high levels in various immune cells such as monocytes, B cells, and naïve T cells (5,8,29,30). CXCR4-knockout mice are embryonically lethal owing to impaired hematopoiesis, organ vascularization, and neuronal migration (29,31). Recent reports have demonstrated that blocking the CXCL12–CXCR4 interaction can inhibit tumor growth by reducing tumor angiogenesis (5,24). Furthermore, inhibition of the CXCL12–CXCR4 pathway in the CD4⁺ T cells of nonobese diabetes (NOD) mice using the specific CXCR4 antagonist AMD3100 can protect against autoimmune diabetes (32). Similarly, administration of AMD3100 reduces the severity of autoimmune lesions in an experimental autoimmune encephalomyelitis model by reducing the number of

immune cells localizing to the perivascular space in response to CXCL12 (33). Autoimmune collagen-induced arthritis in IFN- γ R-deficient DBA/1 mice was reduced in severity by AMD3100 treatment through the inhibition of CXCR4⁺ macrophage migration to target organ (34). Moreover, autoimmune thyroiditis in NOD.H-2^{h4} mice was also suppressed by AMD3100 administration (35). In our study, the autoimmune lesions in *aly/aly* mice were suppressed by AMD3100 administration through the inhibition of TEM cell migration to the target organs. Expression of CXCR4 by naïve T cells in humans is controlled by TGF β signaling [26], and we found that CXCR4 mRNA expression by TEM cells was also enhanced by TGF β 1. Furthermore, the enhancement was strong in the TEM cells of *aly/aly* mice, consistent with the enhanced expression of TGF β R. Collectively, these results suggest that NF- κ B2 may control CXCR4 expression in TEM cells through TGF β signaling.

NIK plays a key role in regulating the processing of p100 to p52 through IKK α in both hematopoietic cells and osteoclasts (10,11,36,37). *NIK*^{-/-} and *aly/aly* mice lack lymph nodes, and, at least for *aly/aly* mice, the T cells show defective proliferation and IL-2 production in response to stimulation by the CD3 antibody (anti-CD3) (13). Furthermore, NIK may be involved in the maintenance of central tolerance in the thymus (14). Moreover, *aly/aly* mice and *RelB*^{-/-} mice show signs of autoimmune disease (16,38). Our previous report demonstrated that NF- κ B2 controls the classical NF- κ B pathway in naïve CD4⁺ T cells by interacting with NF- κ B1 (17). In addition, overactivation of naïve T cells in *aly/aly* mice due to impaired interaction with NF- κ B2 results in induction of the autoimmune reaction (17). In the present study, NF- κ B2

negatively regulated TGF β signaling in TEM cells, while TGF β upregulated CXCR4 expression. It is known that a molecular interaction between NF- κ B2 and Smad3 downstream of TGF β R plays an important role in the transcriptional activity of c-jun (39). Further analysis of the molecular mechanisms controlling CXCR4 expression through NF- κ B2 and TGF β signaling is necessary for understanding how T cells contribute to the pathogenesis of autoimmunity.

Therapy for SS is mainly symptomatic, such as sialogogue or moisturizing agents for dry mouth, and eye drops for dry eye (40). Cytokine or steroid therapy is often effective for some autoimmune diseases such as rheumatoid arthritis. However, a radical therapy for SS has not been established. In *aly/aly* mice, autoimmune lesions were promoted both by upregulation of CXCL12 in the target organs and that of CXCR4 expression on TEM cells. Further study is required to determine the underlying mechanisms for specific CXCL12 overexpression by target tissue but not nontarget tissue such as lung. Inhibiting TEM cell function, including that of autoreactive T cells, may be a promising in the treatment of autoimmune disease. AMD3100 suppresses the growth of several malignant tumors such as prostate cancer and acute myeloid leukemia by inhibiting the CXCR4–CXCL12 axis in tumor stroma. (41,42). Our study identifies numerous potential molecular targets for such interventions.

To summarize, the migratory response of TEM cells to CXCL12 was enhanced in *aly/aly* mice through increased expression of CXCR4 on TEM cells and CXCL12 in the target tissues. Upregulation of CXCL12 in SG and LG suggest that target organs

contribute to the initiation of autoimmunity. Inhibition of CXCL12–CXCR4 signaling in TEM cells could be a useful therapeutic strategy for treating SS. Moreover, CXCR4 expression is regulated by NF-κB2 through TGFβ signaling, revealing additional targets for therapy against autoimmune diseases.

ACKNOWLEDGMENTS

We thank S. Katada, M. Kino, and H. Fukui for technical assistance with support of the mouse colony.

AUTHOR CONTRIBUTIONS

All authors were involved in drafting the article or revising it for important intellectual content, and all authors approved for the final version to be published. Dr. Ishimaru had full access to all of the data in the study and takes responsibility for the integrity of the data and the accuracy of the data analysis.

Study conception and design. Sprent, Ishimaru.

Acquisition of data. Kurosawa, Arakaki, Yamada, Tsunematsu, Kudo.

Analysis of data. Kurosawa, Arakaki.

Writing the paper. Ishimaru.

REFERENCES

1. Masopust D, Schenkel JM. The integration of T cell migration, differentiation and function. *Nat Rev Immunol* 2013;13:309-20.
2. Karin N, Wildbaum G. The Role of Chemokines in Shaping the Balance

- Between CD4(+) T Cell Subsets and Its Therapeutic Implications in Autoimmune and Cancer Diseases. *Front Immunol* 2015;6:609.
3. Armengol MP, Cardoso-Schmidt CB, Fernandez M, Ferrer X, Pujol-Borrell R, Juan M. Chemokines determine local lymphoneogenesis and a reduction of circulating CXCR4+ T and CCR7 B and T lymphocytes in thyroid autoimmune diseases. *J Immunol* 2003;170:6320-8.
 4. Christen U, McGavern DB, Luster AD, von Herrath MG, Oldstone MB. Among CXCR3 chemokines, IFN-gamma-inducible protein of 10 kDa (CXC chemokine ligand (CXCL) 10) but not monokine induced by IFN-gamma (CXCL9) imprints a pattern for the subsequent development of autoimmune disease. *J Immunol* 2003;171:6838-45.
 5. Singh AK, Arya RK, Trivedi AK, Sanyal S, Baral R, Dormond O, Briscoe DM, Datta D: Chemokine receptor trio. CXCR3, CXCR4 and CXCR7 crosstalk via CXCL11 and CXCL12. *Cytokine Growth Factor Rev* 2013;24:41-9.
 6. Antonelli A, Ferrari SM, Giuggioli D, Ferrannini E, Ferri C, Fallahi P. Chemokine (C-X-C motif) ligand (CXCL)10 in autoimmune diseases. *Autoimmun Rev* 2014;13:272-80.
 7. Sanchez-Martin L, Sanchez-Mateos P, Cabanas C. CXCR7 impact on CXCL12 biology and disease. *Trends Mol Med* 2013;19:12-22.
 8. Kremer KN, Clift IC, Miamen AG, Bamidele AO, Qian NX, Humphreys TD, Hedin KE. Stromal cell-derived factor-1 signaling via the CXCR4-TCR heterodimer requires phospholipase C-beta3 and phospholipase C-gamma1 for distinct cellular responses. *J Immunol* 2011;187:1440-7.
 9. Tarnowski M, Grymula K, Reca R, Jankowski K, Maksym R, Tarnowska J, Przybylski G, Barr FG, Kucia M, Ratajczak MZ. Regulation of expression of stromal-derived factor-1 receptors: CXCR4 and CXCR7 in human rhabdomyosarcomas. *Mol Cancer Res* 2010;8:1-14.
 10. Gerondakis S, Fulford TS, Messina NL, Grumont RJ. NF-kappaB control of T cell development. *Nat Immunol* 2014;15:15-25.
 11. Oeckinghaus A, Hayden MS, Ghosh S. Crosstalk in NF-kappaB signaling pathways. *Nat Immunol* 2011;12:695-708.
 12. Yin L, Wu L, Wesche H, Arthur CD, White JM, Goeddel DV, Schreiber RD. Defective lymphotoxin-beta receptor-induced NF-kappaB transcriptional

- activity in NIK-deficient mice. *Science* 2001;291:2162-5.
13. Matsumoto M, Yamada T, Yoshinaga SK, Boone T, Horan T, Fujita S, Li Y, Mitani T. Essential role of NF-kappa B-inducing kinase in T cell activation through the TCR/CD3 pathway. *J Immunol* 2002;169:1151-8.
 14. Mouri Y, Nishijima H, Kawano H, Hirota F, Sakaguchi N, Morimoto J, Matsumoto M. NF-kappaB-inducing kinase in thymic stroma establishes central tolerance by orchestrating cross-talk with not only thymocytes but also dendritic cells. *J Immunol* 2014;193:4356-67.
 15. Noma H, Eshima K, Satoh M, Iwabuchi K. Differential dependence on nuclear factor-kappaB-inducing kinase among natural killer T-cell subsets in their development. *Immunology* 2015;146:89-99.
 16. Tsubata R, Tsubata T, Hiai H, Shinkura R, Matsumura R, Sumida T, Miyawaki S, Ishida H, Kumagai S, Nakao K et al. Autoimmune disease of exocrine organs in immunodeficient alymphoplasia mice: a spontaneous model for Sjogren's syndrome. *Eur J Immunol* 1996;26:2742-8.
 17. Ishimaru N, Kishimoto H, Hayashi Y, Sprent J. Regulation of naive T cell function by the NF-kappaB2 pathway. *Nat Immunol* 2006;7:763-72.
 18. Hamann D, Baars PA, Rep MH, Hooibrink B, Kerkhof-Garde SR, Klein MR, van Lier RA. Phenotypic and functional separation of memory and effector human CD8+ T cells. *J Exp Med* 1997;186:1407-18.
 19. Woodland DL, Kohlmeier JE. Migration, maintenance and recall of memory T cells in peripheral tissues. *Nat Rev Immunol* 2009;9:153-61.
 20. Sallusto F, Lenig D, Forster R, Lipp M, Lanzavecchia A. Two subsets of memory T lymphocytes with distinct homing potentials and effector functions. *Nature* 1999;401(6754):708-12.
 21. Mueller SN, Mackay LK. Tissue-resident memory T cells: local specialists in immune defence. *Nat Rev Immunol* 2016;16:79-89.
 22. Barone F, Bombardieri M, Manzo A, Blades MC, Morgan PR, Challacombe SJ, Valesini G, Pitzalis C. Association of CXCL13 and CCL21 expression with the progressive organization of lymphoid-like structures in Sjögren's syndrome. *Arthritis Rheum* 2005;52:1773-84.
 23. Moriyama M, Hayashida JN, Toyoshima T, Ohyama Y, Shinozaki S, Tanaka A, Maehara T, Nakamura S. Cytokine/chemokine profiles contribute to

- understanding the pathogenesis and diagnosis of primary Sjogren's syndrome. *Clin Exp Immunol* 2012;169:17-26.
24. Wurth R, Bajetto A, Harrison JK, Barbieri F, Florio T. CXCL12 modulation of CXCR4 and CXCR7 activity in human glioblastoma stem-like cells and regulation of the tumor microenvironment. *Front Cell Neurosci* 2014;8:144.
 25. Gorelik L, Flavell RA. Transforming growth factor-beta in T-cell biology. *Nat Rev Immunol* 2002;2:46-53.
 26. Franitza S, Kollet O, Brill A, Vaday GG, Petit I, Lapidot T, Alon R, Lider O: TGF-beta1 enhances SDF-1alpha-induced chemotaxis and homing of naive T cells by up-regulating CXCR4 expression and downstream cytoskeletal effector molecules. *Eur J Immunol* 2002;32:193-202.
 27. Amft N, Bowman SJ. Chemokines and cell trafficking in Sjogren's syndrome. *Scand J Immunol* 2001;54:62-9.
 28. Moriuchi M, Moriuchi H, Turner W, Fauci AS. Cloning and analysis of the promoter region of CXCR4, a coreceptor for HIV-1 entry. *J Immunol* 1997;159:4322-9.
 29. Ma Q, Jones D, Borghesani PR, Segal RA, Nagasawa T, Kishimoto T, Bronson RT, Springer TA. Impaired B-lymphopoiesis, myelopoiesis, and derailed cerebellar neuron migration in CXCR4- and SDF-1-deficient mice. *Proc Natl Acad Sci U S A* 1998;95:9448-53.
 30. Aiuti A, Tavian M, Cipponi A, Ficara F, Zappone E, Hoxie J, Peault B, Bordignon C. Expression of CXCR4, the receptor for stromal cell-derived factor-1 on fetal and adult human lympho-hematopoietic progenitors. *Eur J Immunol* 1999;29:1823-31.
 31. Tachibana K, Hirota S, Iizasa H, Yoshida H, Kawabata K, Kataoka Y, Kitamura Y, Matsushima K, Yoshida N, Nishikawa S et al. The chemokine receptor CXCR4 is essential for vascularization of the gastrointestinal tract. *Nature* 1998;393:591-4.
 32. Aboumrad E, Madec AM, Thivolet C. The CXCR4/CXCL12 (SDF-1) signalling pathway protects non-obese diabetic mouse from autoimmune diabetes. *Clin Exp Immunol* 2007;148:432-9.
 33. McCandless EE, Wang Q, Woerner BM, Harper JM, Klein RS. CXCL12 limits inflammation by localizing mononuclear infiltrates to the perivascular space

- during experimental autoimmune encephalomyelitis. *J Immunol* 2006;177:8053-64.
34. Matthys P, Hatse S, Vermeire K, Wuyts A, Bridger G, Henson GW, De Clercq E, Billiau A, Schols D. AMD3100, a potent and specific antagonist of the stromal cell-derived factor-1 chemokine receptor CXCR4, inhibits autoimmune joint inflammation in IFN-gamma receptor-deficient mice. *J Immunol* 2001;167:4686-92.
 35. Liu X, Mao J, Han C, Peng S, Li C, Jin T, Fan C, Shan Z, Teng W. CXCR4 antagonist AMD3100 ameliorates thyroid damage in autoimmune thyroiditis in NOD.H2h(4) mice. *Mol Med Rep* 2016;13:3604-12.
 36. Sanchez-Valdepenas C, Punzon C, San-Antonio B, Martin AG, Fresno M. Differential regulation of p65 and c-Rel NF-kappaB transactivating activity by Cot, protein kinase C zeta and NIK protein kinases in CD3/CD28 activated T cells. *Cell Signal* 2007;19:528-37.
 37. Novack DV, Yin L, Hagen-Stapleton A, Schreiber RD, Goeddel DV, Ross FP, Teitelbaum SL. The IkappaB function of NF-kappaB2 p100 controls stimulated osteoclastogenesis. *J Exp Med* 2003;198:771-81.
 38. Burkly L, Hession C, Ogata L, Reilly C, Marconi LA, Olson D, Tizard R, Cate R, Lo D. Expression of relB is required for the development of thymic medulla and dendritic cells. *Nature* 1995;373:531-6.
 39. Lopez-Rovira T, Chalaux E, Rosa JL, Bartrons R, Ventura F. Interaction and functional cooperation of NF-kappa B with Smads. Transcriptional regulation of the junB promoter. *J Biol Chem* 2000;275:28937-46.
 40. Barone F, Colafrancesco S. Sjogren's syndrome: from pathogenesis to novel therapeutic targets. *Clin Exp Rheumatol* 2016;34:58-62.
 41. Domanska UM, Timmer-Bosscha H, Nagengast WB, Oude Munnink TH, Kruizinga RC, Ananias HJ, Kliphuis NM, Huls G, De Vries EG, de Jong IJ et al. CXCR4 inhibition with AMD3100 sensitizes prostate cancer to docetaxel chemotherapy. *Neoplasia* 2012;14:709-18.
 42. Kim HY, Lee SY, Kim DY, Moon JY, Choi YS, Song IC, Lee HJ, Yun HJ, Kim S, Jo DY. Expression and functional roles of the chemokine receptor CXCR7 in acute myeloid leukemia cells. *Blood Res* 2015;50:218-26.

Figure legends

Figure 1. Inflammatory lesions associated with infiltration of effector memory T (TEM) cells into the target organs of *aly/aly* autoimmune model mice (12 weeks). **A**, Inflammatory lesions in the salivary glands (SGs) of female *aly/aly* mice at 3 months of age. Scale bar, 50 μ m. **B**, Accumulation of CD4 $^{+}$ T cells in the SGs of *aly/aly* mice as detected using immunofluorescence staining. Scale bar, 20 μ m. The photos are representative of each group. **C**, CD4 $^{+}$ and CD8 $^{+}$ subsets of lymphocytes infiltrated into the SGs of *aly/aly* and *aly/+* mice as detected by flow cytometry. **D**, Number of CD4 $^{+}$ and CD8 $^{+}$ T cells among the infiltrated lymphocytes in the SGs of *aly/aly* and *aly/+* mice. Data are shown as average \pm standard deviation (SD) of six to eight mice per group. * p < 0.05. **E**, CD44/CD62L expression in CD4 $^{+}$ T cells in the spleen and SGs of *aly/aly* and *aly/+* mice as detected using flow cytometry. The results are representative of each group. **F**, Numbers of CD44 $^{\text{high}}$ CD62L $^{-}$ TEM and CD44 $^{\text{low}}$ CD62L $^{+}$ naïve CD4 $^{+}$ cells in the spleen and SGs of *aly/aly* and *aly/+* mice. Data are shown as average \pm SD of six to eight mice per group. * p < 0.05.

Figure 2. Enhanced migratory rate of TEM cells toward CXCL12 isolated from *aly/aly* mice (12 weeks). **A**, Chemotactic activities of TEM cells in the presence of CXCL9, 10, 11, and 12 (all 750 ng/ml) were analyzed by *in vitro* migration assay with transwell membranes (3 μ m). The data are expressed as average \pm SD of triplicates, and are representative of three independent experiments. * p < 0.05. **B**, Chemotactic activity of naïve CD4 $^{+}$ T cells in the presence of CXCL9, 10, 11, and 12. **C**, Dose-dependent

migratory response of CD4⁺ TEM cells to CXCL12 (250, 500, and 750 ng/ml) in *aly/aly* mice. Data are shown as average ± SD of triplicates and are representative of three independent experiments. **p* < 0.05. **D**, Migratory response of naïve CD4⁺ T cells to CXCL12. All data presented as average ± SD of three independent experiments conducted in triplicate.

Figure 3. CXCL12 overexpression in target tissues of *aly/aly* mice (16 weeks). **A**, CXCL12 concentration in sera from B6, *aly/+*, and *aly/aly* mice as determined by ELISA. Data are shown as average ± SD of four mice per group. **B**, CXCL12 mRNA expression levels in the spleen, SG, LG, and lung as analyzed by qRT-PCR. Data are shown as average ± SD of five mice per group. **p* < 0.05. **C**, CXCL12 expression in LGs in *aly/aly* and *aly/+* mice as detected by immunofluorescence analysis using Alexa-546-conjugated anti-EpCAM mAb and Alexa-488-conjugated anti-CXCL12 mAb. The nuclei were stained with DAPI. The results were representative of five mice per group. Scale bar, 10 μm. Lymphocyte (Ly) infiltrating area was separated from epithelial cell (Ep) area by white dot line. **D**, Immunofluorescence analysis of LGs was performed with Alexa-546-conjugated anti-Ly5.2 mAb and Alexa-488-conjugated anti-CXCL12 mAb. The nuclei were stained with DAPI. The results were representative of five mice per group. Scale bar, 10 μm. Ly infiltrating area was separated from Ep area by white dot line. The results were representative of five mice per group.

Figure 4. Overexpression of CXCR4 and CXCR7 in *aly/aly* TEM cells. **A** and **B**, Cell

surface expression of CXCR7 and CXCR4 in TEM cells (**A**) and naïve (**B**) CD4⁺ T cells from the spleen of *aly/aly* and *aly/+* mice (10 weeks) was detected by flow cytometry. Expression relative to isotype control detected as mean fluorescence intensity (MFI) and presented as average ± SD of five mice per group. **p* < 0.05. **C** and **D**, mRNA expression of CXCR7 and CXCR4 in TEM (**C**) and naïve (**D**) CD4⁺ T cells in the spleen of *aly/+* and *aly/aly* mice as analyzed by qRT-PCR. Data are shown as average ± SD of seven mice per group. **p* < 0.05. **E** and **F**, Migratory response to CXCL12 (750 ng/ml) of TEM (**E**) and naïve (**F**) CD4⁺ T cells in the spleen of WT, *NF-κB1*^{-/-}, *aly/aly*, and *RelB*^{-/-} mice (10 weeks). Data are shown as average ± SD of three independent experiments conducted in triplicate. **p* < 0.05, ***p* < 0.05.

Figure 5. Enhanced CXCL12-induced migration of TEM cells by activation of TGFβ signaling. **A**, CD4⁺ TEM and naïve CD4⁺ T cells of *aly/aly* and *aly/+* mice (10–12 weeks) were stimulated with TGFβ1 (0.125 ng/ml) for 24 h. CXCR4 mRNA expression determined by qRT-PCR. Data are shown as average ± SD of five mice per group. **p* < 0.05, ***p* < 0.005. **B**, Cell surface expression of CXCR4 in TEM and naïve CD4⁺ T cells from the spleen of *aly/aly* and *aly/+* mice was detected by flow cytometry. Expression relative to isotype control detected as MFI and presented as average ± SD of five mice per group. **p* < 0.05, ***p* < 0.005. **C**, TEM cells from *aly/aly* and *aly/+* mice were stimulated with TGFβ1 (0.125 ng/ml) or sham-treated for 24 h and the migratory response to CXCL12 (750 ng/ml) as analyzed by *in vitro* migration assay. Data are shown as average ± SD of three independent experiments conducted in triplicate. **p* <

0.05. **D**, mRNA expression of TGF β RI, II, and III in naïve and TEM cells from *aly/aly* and *aly/+* mice were determined by qRT-PCR. Data are shown as average \pm SD of five mice per group. * p < 0.05. **E**, TGF β RI $^+$ TEM and naïve CD4 $^+$ T cells were analyzed by flow cytometry. Data are shown as average \pm SD of five mice per group. ** p < 0.005. **F**, TGF β RII $^+$ TEM and naïve CD4 $^+$ T cells were analyzed by flow cytometry. Data are shown as average \pm SD of five mice per group. * p < 0.05.

Figure 6. Therapeutic effect of a CXCR4 inhibitor on autoimmune lesions in *aly/aly* mice. The CXCR4 inhibitor (AMD3100, 5 mg/kg) was intraperitoneally injected daily into *aly/aly* mice from 8 to 16 weeks of age. **A** and **B**, Paraffin-embedded sections of SG (**A**) and LG (**B**) from control and AMD3100-administered mice stained with H&E. Photos are representative of five mice for each group. Scale bar: 50 μ m. **C** and **D**, Numbers of TEM and naïve CD4 $^+$ T cells among infiltrated lymphocytes in SG (**C**) and LG (**D**) of control and AMD3100-treated mice were determined by flow cytometry. Data are shown as average \pm SD of five mice per group. * p < 0.05.

Figure 1

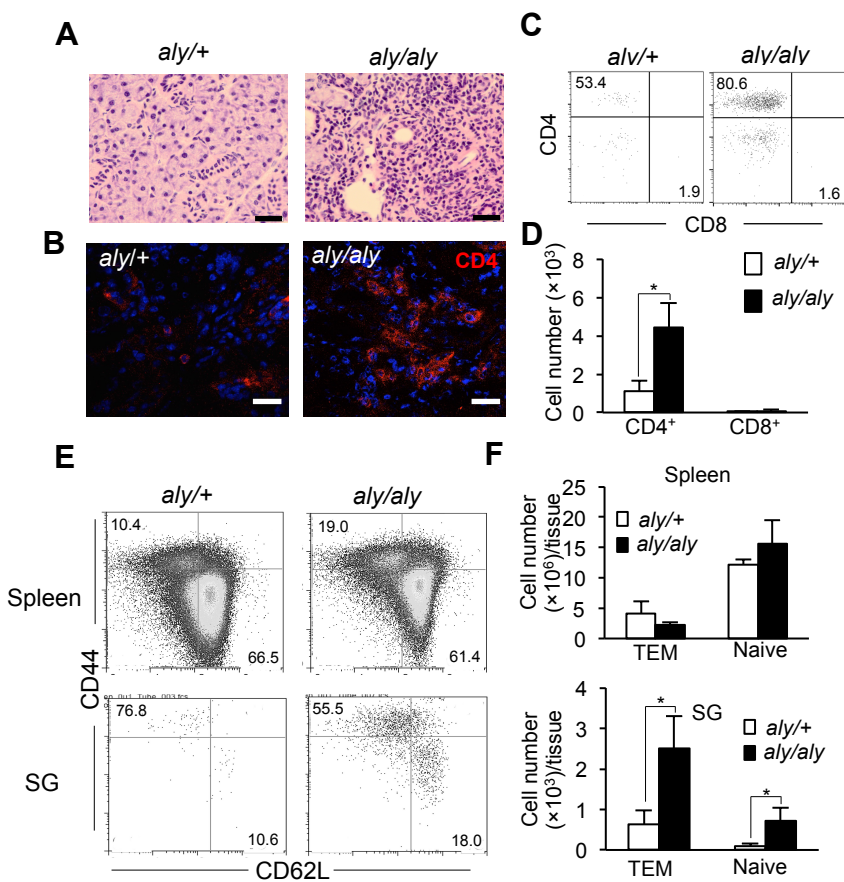


Figure 2

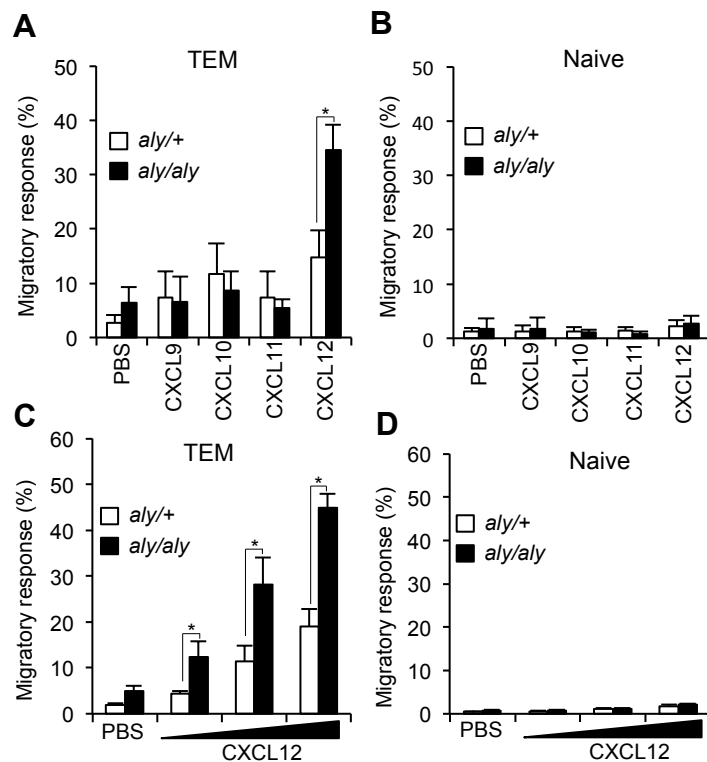


Figure 3

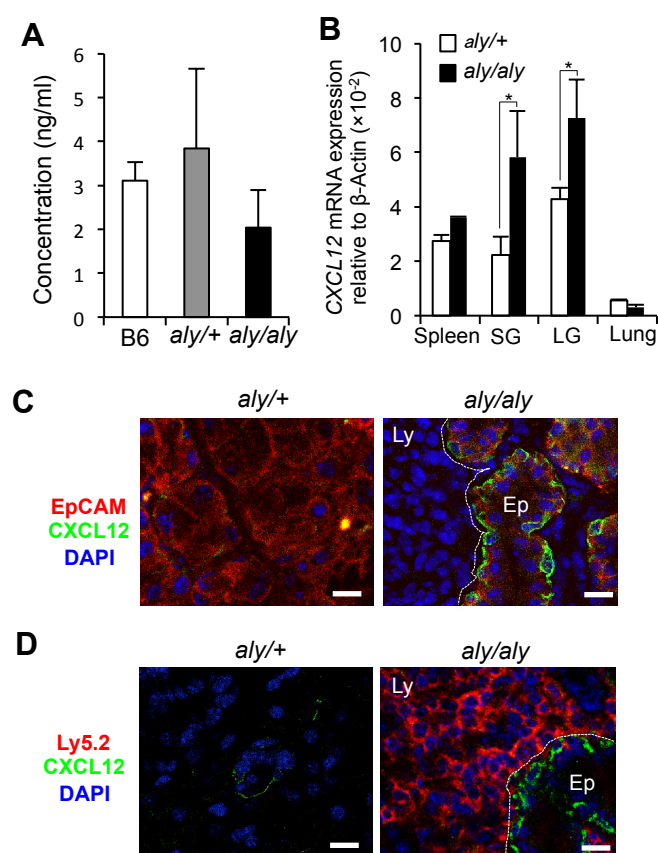


Figure 4

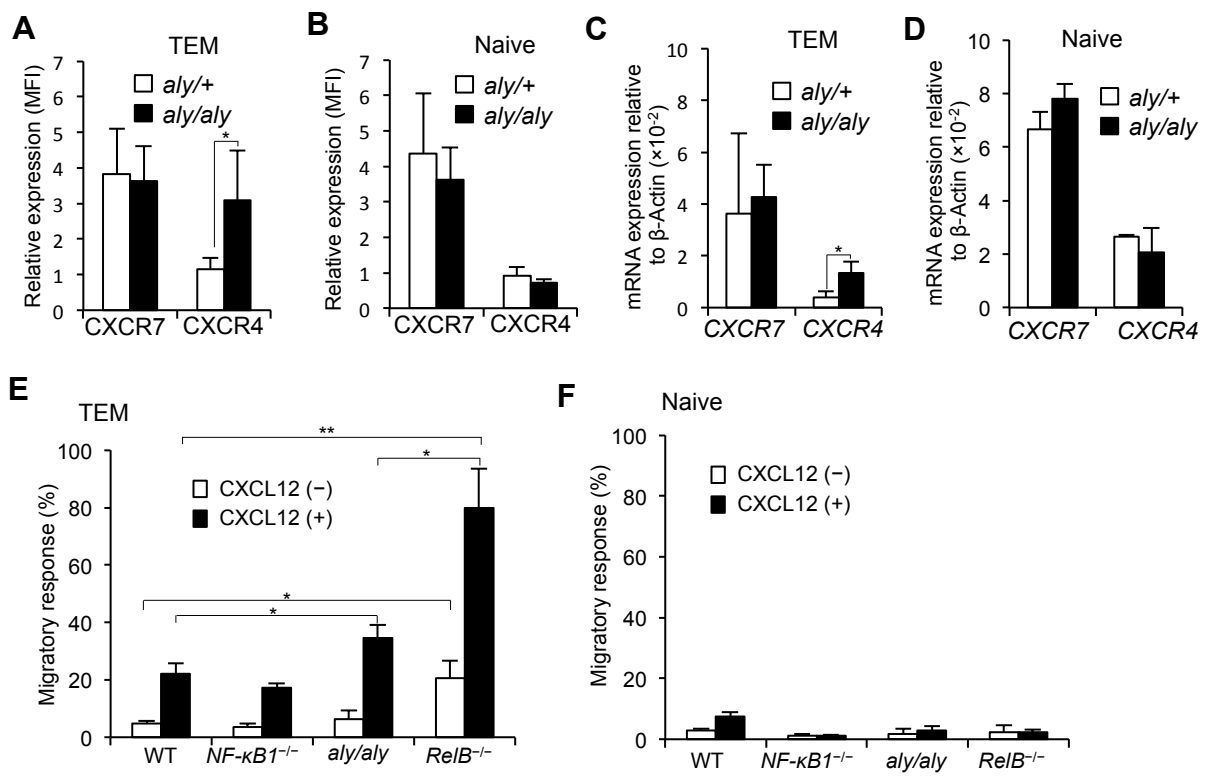


Figure 5

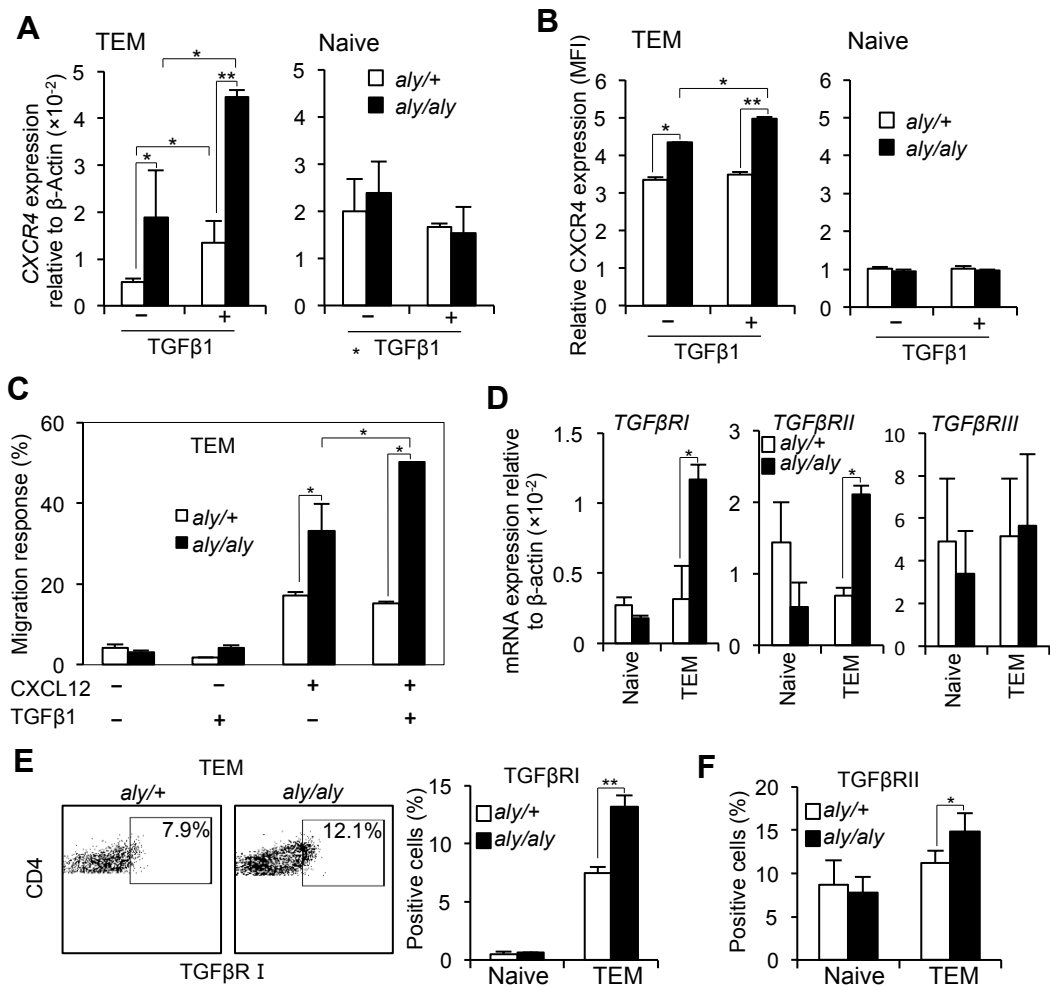


Figure 6

